Magnetic properties and interfacial anisotropies of Pt / Co / AlOx perpendicularly magnetized thin films

R Mansell, A Mizrahi, A Beguivin and RP Cowburn

Cavendish Laboratory, University of Cambridge, JJ Thomson Avenue, Cambridge, CB3 0HE, UK

Abstract

Thin films of Pt/Co/AlO_x, showing perpendicular magnetic anisotropy, were grown by magnetron sputtering with the AlO_x formed by oxidation of thin Al layers using an oxygen atom source. Films were studied as a function of Pt thickness and Al oxidation and films which showed full remanence and sharp switching coercive were achieved. In order to prevent further oxidation of the interface in ambient conditions we use a double Al growth and oxidation process. Magneto optical Kerr effect and vibrating sample magnetometry were used to analyse these films. We find an effective perpendicular anisotropy of 2.0 x 10^6 erg/cm^3, with the majority of the perpendicular anisotropy coming from the Pt/Co interface. From the sweep rate dependence of the coercivity we are able to extract an activation volume of 4.3 ± 0.5 x 10^{-18} cm^3, similar to other Co-based perpendicular systems.

1. Introduction

The recent discovery of novel spin orbit torque effects in systems with either a heavy metal in contact with a magnetic layer or an interface between a magnetic layer and an oxide has led to an intensive research effort studying asymmetric magnetic multilayers [1,2,3]. Different origins of the torques have been proposed, coming from spin injection into the ferromagnetic layer due to the spin Hall effect in the heavy metal underlayer [2,3], or from the Rashba effect across the ferromagnetic/oxide interface [1,4]. Recent work has attempted to disentangle the sources of these torques and generalize their forms [4]. The interest in these materials comes both from the discovery of novel spin-dependent behaviour, as well as the possibility of exploiting these for new commercially-relevant devices. Spin-orbit torque driven memory [5] and logic devices [6] have been proposed which appear to have lower operating currents than STT MRAM devices [5]. Since these effects are current driven, both the heavy metal underlayers as well as the metal/oxide heterointerfaces need to be optimized [7]. Switching of magnetic layers via current may also provide a way of injecting data into nanomagnetic logic schemes, which are driven by magnetic field or current pulses [8,9,10]. The separation of the injection of data from the means of controlling the logic gates themselves is advantageous because it leads to larger device operating margins.

One important discovery in a Pt/Co/AlO_x system is that of high domain wall velocities [11]. This is due to a combination of both the spin-orbit torque induced motion and the Dzyaloshinskii-Moriya interaction [12]. The Dzyaloshinskii-Moriya interaction is a chiral interaction that can occur in thin film systems due to a combination of spin-orbit coupling and broken symmetry at the interface [13,14]. The Pt/Co/AlO_x system has been shown to lead to a large Dzyaloshinskii-Moriya interaction [15,16]. It has also been shown that a voltage applied across the AlO_x can induce pinning in domain walls, due to local changes in the anisotropy induced by the electric field [17].

This makes Pt/Co/AlO_x an important model system which also has the advantage of consisting of relatively well-understood elements: Pt and Co form a standard perpendicular

anisotropy system and AlO_x growth has been widely studied due to its relevance as a tunnel barrier [18]. In this paper we study the effects of oxidation of the AlOx and the Pt underlayer thickness in $Pt/Co/AlO_x$ perpendicularly magnetized multilayers, in particular looking at the relative contributions of the two interfaces to the perpendicular anisotropy, as a step towards usage in nanomagnetic devices.

2. Sample growth

Pt/Co/Al trilayers were magnetron sputtered at room temperature in a system with a base pressure of $3x10^{-8}$ mbar onto substrates with a native silicon oxide. The sputter powers were 100 W for the Pt, 60 W for the Co and 50 W for the Al, at an Ar pressure of 8×10^{-3} mbar followed by oxidation of the Al layers by an oxygen atom source. The atom source creates a plasma using a microwave magnetron and is fitted with a low conductance aperture which provides unionized oxygen atoms at thermal energies. Previous $Pt/Co/AlO_x$ studies have mainly used rf sources to provide an oxygen plasma [19,20]. The atom source is located in the load-lock of the main system which has a base pressure of 1×10^{-7} mbar. All films were oxidized at a constant O_2 chamber pressure of 6×10^{-5} mbar with a 25 mA magnetron current. With a fixed pressure and current, the optimization of the oxidation of the Al layer can be studied in two ways. Firstly, Al layers of different thickness can be grown and then oxidized for a set time. Secondly for a fixed thickness Al layer the oxidation time can be varied. The first approach is demonstrated in figure 1, using a Pt (4 nm)/Co (0.6 nm)/Al (t) stack, where, for the films which are oxidized by the atom source, the oxidation time is fixed at 1 min. Initially, a sample with a naturally oxidized 2 nm Al film is measured by polar magneto-optical Kerr effect (MOKE) magnetometry under an applied perpendicular field which shows a hard axis loop saturating around 800 Oe. For a 2 nm film that undergoes 1 min of oxidation we see a slight decrease in the out-of-plane saturation to around 600 Oe. This suggests that very little oxygen is reaching the interface through the 2 nm film. As the thickness of the Al layer is reduced we see fully

remanent perpendicular hysteresis loops between 1.2 nm and 1.5 nm Al before the films show a slanted in-plane type loop for thinner Al. This shows how the oxidation of the film reached the Co/Al interface, which leads to maximized perpendicular anisotropy before leading to the oxidation of the Co [19,20,21]. We found that when growing 1.5 nm of Al or more we were unable to oxidize the film to an equivalent state as seen for the 1.3 nm film, even with 10 min oxidation time. This is consistent with previous reports showing an exponential change of oxidation time with Al thickness [22]. This restricts this technique to thin Al layers. However, at atmospheric pressure the limiting oxide thickness in Al is around 2 nm. Therefore, using Al layers of around 1 nm means that the devices will not survive in air for a long period of time. Eventually the Al layer will fully oxidize along with the Co layer underneath, something seen experimentally with the loss of magnetization of the samples over time. To overcome this problem we sequentially sputter and oxidize two layers of Al which leads to a total thickness of oxide which does not lead to further penetration of oxygen to the Co interface when exposed to air.

For spin orbit torque devices there are three considerations which can determine the PT layer thickness. Firstly, the Co/Pt interface provides perpendicular anisotropy. Secondly, in order to achieve high current densities and so maximize the possibility of observing current driven effects, this layer should be as thin as possible. Thirdly, however, the size of any spin Hall effect from this layer should be maximized. This third part requires knowledge about the spin diffusion length in Pt. Recent experiments have shown that in sputtered Pt, where the resistivity is higher than in MBE grown or foil samples the spin diffusion length can be very low. A typical value of 1.4 nm has been suggested and values as low as 0.5 nm have been reported [23]. This means that an optimized Pt underlayer should be as thin as possible but not thinner than around 1.5 nm. In figure 2 polar MOKE loops are shown with three samples with differing Pt underlayer thickness. For 3 nm Pt thickness (figure 2(a)) we have a fully perpendicular anisotropy with full remanence. For 2.5 nm (figure 2(b)) the film is still perpendicular but has slightly less than full remanence whilst for the 2 nm (figure 2(c)) Pt film we see that the loop is heavily slanted, suggesting the loss of perpendicular anisotropy. This

shows how the Pt underlayer is important in providing perpendicular anisotropy to the system. The thinner Pt layers have lower interface anisotropies as the (111) texture which maximizes the perpendicular anisotropy has not fully developed. In this case the loss of perpendicular anisotropy occurs for thicker layers than the likely spin diffusion limit. This is an important difference between Pt/Co/AlOx and systems where the magnetic layer contains Fe which can be perpendicular just from the magnetic metal/oxide interface [7].

3.1 Magnetic properties of an optimized film

Figure 3 shows magnetic hysteresis loops taken by vibrating sample magnetometry (VSM) of a Pt (4 nm)/ Co (0.8 nm) / AlO_x film, where the AlOx was formed by two steps of 1.3 nm Al followed by 1 min of oxidation. The measurements shown here were taken a year after the sample was grown, having been stored in air. In figure 3(a), with the field applied perpendicularly to the film there is an easy axis loop with 100 % remanence with a switching field of around 75 Oe. Applying the field in the film plane (figure 3(b)) a clear hard axis loop is seen with a saturation field of 6 kOe. The hard axis curve is not particularly sharp in the transition from saturation which may suggest some inhomogeneity across the ~0.5 cm^2 sample. This may originate from the relatively small beam size of the atom source which has a 1 cm diameter aperture. From these loops a saturation magnetization, M_s, of 650 ± 50 emu/cm^3 can be extracted. This is significantly lower than the bulk M_s of Co, 1400 emu/cm^3, but in line with other measurements on this system where an M_s of 800 emu/cm^3 has been reported [19]. The reduction may come from interfacial intermixing with the Pt at the bottom interface and slight oxidation at the top. Using the saturation field, H_K, as well as M_s, the effective anisotropy of the Co layer, $K_{eff} = H_K \frac{M_s}{2}$, can be calculated, giving a value of 2.0 x 10^6 erg/cm^3. Furthermore, the total interfacial uniaxial anisotropy can be estimated from $K_{eff} = K_1/t + K_v$, with K_1 the interfacial uniaxial anisotropy, t the thickness, and K_v the volume anisotropy of Co. Using an average literature value for the volume anisotropy of Co, K_v = -9 x 10^6 erg/cm^3 [24], which

corresponds to that found in similar thin films, and is between the bulk values expected for fcc and hcp lattices, we find an interface anisotropy for both interfaces of 0.88 erg/cm^2. One interesting question for these types of multilayers is the contributions of the top and bottom surfaces to the interface anisotropy. It has been shown in Pt/Co/Pt systems that the majority of the anisotropy is actually from the bottom interface, due to the greater intermixing of Pt grown on Co, than of Co grown on Pt [25]. From the total interfacial anisotropy and the hard axis out-of-plane saturation from the 2 nm Al unoxidized sample (in figure 1) we can estimate the relative contributions to the interface anisotropy from the Pt/Co and Co/AlOx interfaces. The 2 nm unoxidized sample, which has a 0.6 nm Co layer, shows in-plane anisotropy and saturates out-of-plane at around 800 Oe. Assuming that a Co/Al interface provides no out-of-plane anisotropy, we can estimate that the bottom interface provides 8.7 x 10^6 erg/cm^3 of the total anisotropy which is equivalent to an interfacial anisotropy of 0.52 erg/cm^2 [25,29]. Therefore, the Co/AlOx interface is providing around 0.36 erg/cm^2 of perpendicular interfacial anisotropy [19]. This gives only an approximation of the anisotropies due to the assumption that go into the calculation, including that of no anisotropy contribution from a Co/Al interface. Similar Pt/Co systems with only one contributing interface show perpendicular magnetization indicating the strength of this interfacial term [25,30]. We see that even in an as-grown system the Co/AlOx interface is able to achieve significant perpendicular interfacial anisotropy. Whilst larger interfacial anisotropies may be obtainable through annealing Co/oxide interfaces, this may affect other layers in a multilayer system, degrading the performance of the device as a whole. Control of the relative ratios of the top and bottom anisotropies could allow tuning of such effects as spin orbit torques, Dzyaloshinskii-Moriya interaction or voltage controlled anisotropy [1,26,27]. Understanding how the interfacial anisotropy and other interfacial effects are related to each other is an important step for the optimization of devices.

3.2 Rate Dependence of the coercivity

The rate dependence of the coercivity of the 0.8 nm Co film characterized above has also been measured, shown in figure 4. The coercive field of the sample is plotted as a function of the natural log of the sweep rate. This plot shows, as is seen in other perpendicular anisotropy films, two distinct regions of rate dependence [31], marked by the continuous and dashed lines in the figure. The reversal at lower sweep rates is due to nucleation of a small number of domains which then expand across the sample. At higher sweep rates the reversal is dominated by the nucleation of new domains [32,33]. This is also associated with a slanting of the hysteresis loop. From the lower sweep rate linear regime we can fit the line with the equation [31]:

$$H_c = \left[\ln\left(\dot{H}\right) + \ln\left(ln2 \times t_{H=0} \times \frac{V^* M_S}{k_B T}\right)\right] \times \frac{k_B T}{V^* M_S}$$

Where H_c is the coercivity, $\dot{H}$ is the field sweep rate, $t_{H=0}$ is the magnetic decay time, V^* is the activation volume, k_B the Boltzmann constant and T the temperature. From the graph we extract a slope of 14.9 ± 0.7 Oe and an intercept of 44 ± 4 Oe. Using M_s from the VSM measurement and the slope and intercept of the graph allows us to determine V^* = 4.3 ± 0.5 x 10^{-18} cm^3 and $t_{H=0}$ = 385 s. The activation volume is similar to those quoted elsewhere for perpendicular Co layers [31,32,34]. The activation volume has a related length scale, found by $l^* = \sqrt{\frac{V^*}{t}}$, where t is the sample thickness, which we find to be 85 nm. It is notable that in these perpendicular films this characteristic length scale becomes quite large such that it is easy to pattern elements which are around this critical length, which would be expected to cause a change in the magnetic properties of the layer [35,36].

4. Conclusion

We have grown perpendicularly magnetized Pt/Co/AlO_x films, making the AlO_x using an atom source to oxidize thin Al films. We find that a double Al film and oxidation step is necessary to create AlO_x thick enough to protect the Co from oxidation. By deducing the effect of an optimally oxidized AlO_x

layer on the perpendicular anisotropy we show that the Pt/Co interface is responsible for most of the perpendicular anisotropy. We use the rate dependence of the coercivity to extract the activation volume which is comparable to other perpendicular Co systems. The results highlight the importance of understanding the different interface effects in such asymmetric magnetic multilayers which can be optimized to make them suitable for use in novel nanomagnetic devices.

Acknowledgements

This research is funded by the European Community under the Seventh Framework Program ERC Contract No. 247368: 3SPIN. AB acknowledges DTA funding from the EPSRC.

References

[1] I. M. Miron, G. Gaudin, S. Auffret, B. Rodmacq, A. Schuhl, S. Pizzini, J. Vogel, and P. Gambardella, *Nature Materials* **9**, 230 (2010)

[2] L. Liu, C.-F. Pai, Y. Li, H. W. Tseng, D. C. Ralph, and R. A. Buhrman, *Science* **336**, 555 (2012)

[3] P. P. J. Haazen, E. Murè, J. H. Franken, R. Lavrijsen, H. J. M. Swagten, and B. Koopmans, *Nature Materials* **12**, 299 (2013)

[4] K. Garello, I. M. Miron, C. O. Avci, F. Freimuth, Y. Mokrousov, S. Blügel, S. Auffret, O. Boulle, G. Gaudin, and P. Gambardella, *Nature Nanotechnology* **8**, 587 (2013)

[5] I. M. Miron, K. Garello, G. Gaudin, P.-J. Zermatten, M. V. Costache, S. Auffret, S. Bandiera, B. Rodmacq, A. Schuhl, and P. Gambardella, *Nature* **476**, 189 (2011)

[6] D. Bhowmik, L. You and S. Salahuddin, *Nature Nanotechnology* **9**, 59 (2014)

[7] S. Emori, U. Bauer, S.-M. Ahn, E. Martinez, and G. S. D. Beach, *Nature Materials* **12**, 611 (2013)

[8] R. Lavrijsen, J.-H. Lee, A. Fernández-Pacheco, D. C. M. C. Petit, R. Mansell, and R. P. Cowburn, *Nature* **493**, 647 (2013)

[9] J.H. Lee, D. Petit, R. Lavrijsen, A. Fernández-Pacheco, R. Mansell, and R.P. Cowburn, Appl. Phys. Lett. **104** 232404 (2014)

[10] R. Lavrijsen, D. C. M. C. Petit, A. Fernández-Pacheco, J. Lee, R. Mansell, and R. P. Cowburn, *Nanotechnology*, **25** 105201 (2014)

[11] T.A. Moore, I.M. Miron, G. Gaudin, G. Serret, S. Auffret, B. Rodmacq, A. Schuhl, S. Pizzini, J. Vogel, and M. Bonfim, *Appl. Phys. Lett.* **93**, 262504 (2008)

[12] E. Martinez, S. Emori, and G. S. D. Beach, *Appl. Phys. Lett.* **103**, 072406 (2013)

[13] A. Crepieux and C. Lacroix, *J. Magn. Magn. Mat.* **182**, 341349 (1998)

[14] D. Petit, P. R. Seem, M. Tillette, R. Mansell, and R. P. Cowburn, *Appl. Phys. Lett*. **106**, 022402 (2015)

[15] J. H. Franken, M. Herps, H. J. M. Swagten, and B. Koopmans, *Scientific Reports* **4**, 5248 (2014)

[16] S. Pizzini, J. Vogel, S. Rohart, L. D. Buda-Prejbeanu, E. Jué, O. Boulle, I. M. Miron, C. K. Safeer, S. Auffret, G. Gaudin, and A. Thiaville, *Phys. Rev. Lett.* **113**, 047203 (2014)

[17] A. J. Schellekens, A. Van den Brink, J.H. Franken, H.J.M. Swagten, and B. Koopmans, *Nature Communications* **3**, 847 (2012)

[18] W. H. Rippard, A. C. Perrella, F. J. Albert, and R. A. Buhrman, *Phys. Rev. Lett.* **88**, 046805 (2002)

[19] Y. Dahmane, S. Auffret, U. Ebels, B. Rodmacq, and B. Dieny, *IEEE Transactions on Magnetics*, **44**, 2865 (2008)

[20] A. J. Schellekens, L. Deen, D. Wang, J. T. Kohlhepp, H. J. M. Swagten, and B. Koopmans, *Appl. Phys. Lett.* **102**, 082405 (2013)

[21] A. Manchon, C. Ducruet, L. Lombard, S. Auffret, B. Rodmacq, B. Dieny, S. Pizzini, J. Vogel, V. Uhlí, M. Hochstrasser, and G. Panaccione, *Journal of Applied Physics* **104**, 043914 (2008)

[22] S. Monso, B. Rodmacq, S. Auffret, G. Casali, F. Fettar, B. Gilles, B. Dieny, and P. Boyer, *Appl. Phys. Lett.* **80**, 4157 (2002)

[23] L. Liu, R. A. Buhrman, and D. C. Ralph, arXiv:1111.3702 (2012)

[24] M. T. Johnson, P. J. H. Bloemen, F. J. A. den Broeder, and J. J. de Vries, *Rep. Prog. Phys.* **59** 1409 (1996)

[25] S. Bandiera, R. C. Sousa, B. Rodmacq, and B. Dieny, *IEEE Magnetics Letters* **2**, 3000504 (2011)

[26] S. E. Barnes, J. Ieda, and S. Maekawa, *Scientific Reports* **4**, 4105 (2014)

[27] K. L. Wang, J. G. Alzate, and P. Khalili Amiri, *J. Phys. D: Appl. Phys*. **46** 074003 (2013)

[28] A. Hrabec, N. A. Porter, A. Wells, M. J. Benitez, G. Burnell, S. McVitie, D. McGrouther, T. A. Moore, and C. H. Marrows*, Phys. Rev. B* **90**, 020402(R) (2014)

[29] Z. Zhang, P. E. Wigen, and S. S. P. Parkin, *J. Appl. Phys.* **69**, 5649 (1991)

[30] T. Y. Lee, Y. C. Won, D. S. Son, S. H. Lim, and S.-R. Lee, *IEEE Magnetics Letters* **5**, 1000104 (2014)

[31] P. Bruno, G. Bayreuther, P. Beauvillain, C. Chappert, G. Lugert, D. Renard, J. P. Renard, and J. Seiden, *J. Appl. Phys.* **68**, 5759 (1990)

[32] B. Raquet, R. Mamy, and J. C. Ousset, *Phys. Rev. B* **54**, 4128 (1996)

[33] A. Fernández-Pacheco, F. C. Ummelen, R. Mansell, D. Petit, J. H. Lee, H. J. M. Swagten, and R. P. Cowburn, *Appl. Phys. Lett.* **105**, 092408 (2014)

[34] A. Kirilyuk, J. Ferré, V. Grolier, J.P. Jamet, and D. Renard, *J. Magn. Magn. Mat.* **171**, 45 (1997)

[35] K.-J. Kim, J.-C. Lee, S.-M. Ahn, K.-S. Lee, C.-W. Lee, Y. J. Cho, S. Seo, K.-H. Shin, S.-B. Choe, and H.-W. Lee, *Nature* **458**, 740 (2009)

[36] R. Mansell, A. Beguivin, D.C.M.C. Petit, A. Fernández-Pacheco, J.H. Lee, and R.P. Cowburn, *Appl. Phys. Lett.* **107** 092405 (2015)

Figure 1. Polar MOKE loops under perpendicular fields of Pt (4 nm) / Co (0.6 nm) / Al (t) films for 1 min oxidation time. The loops are offset for clarity.

Figure 2. Polar MOKE loops under perpendicular fields for Pt (t) / Co (0.6 nm) / AlOx, for t = (a) 3 nm, (b) 2.5 nm, (c) 2 nm.

Figure 3. (a) Easy axis and (b) hard axis loops of a Pt (4 nm) / Co (0.8 nm) / AlOx sample taken by VSM.

Figure 4. Field sweep rate dependence of the coercivity of the sample measured in figure 3. The unbroken and dashed lines show the two switching regimes seen in the film.

Figure 1.

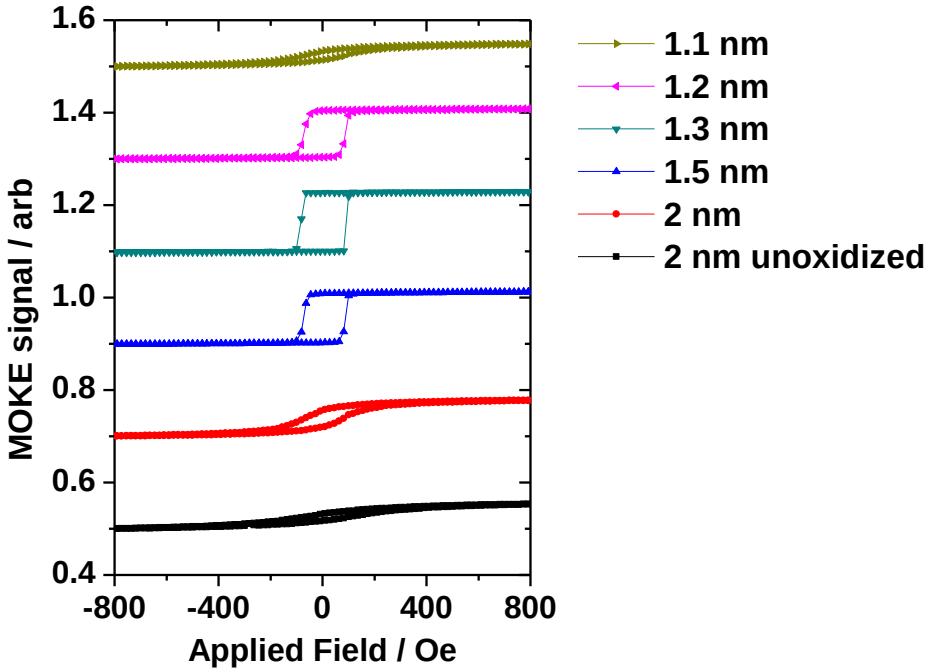

Figure 2.

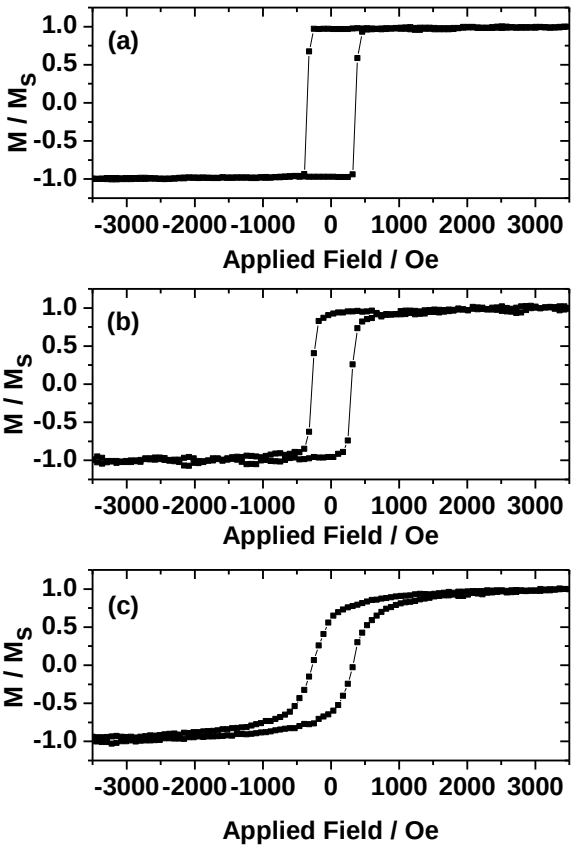

Figure 3.

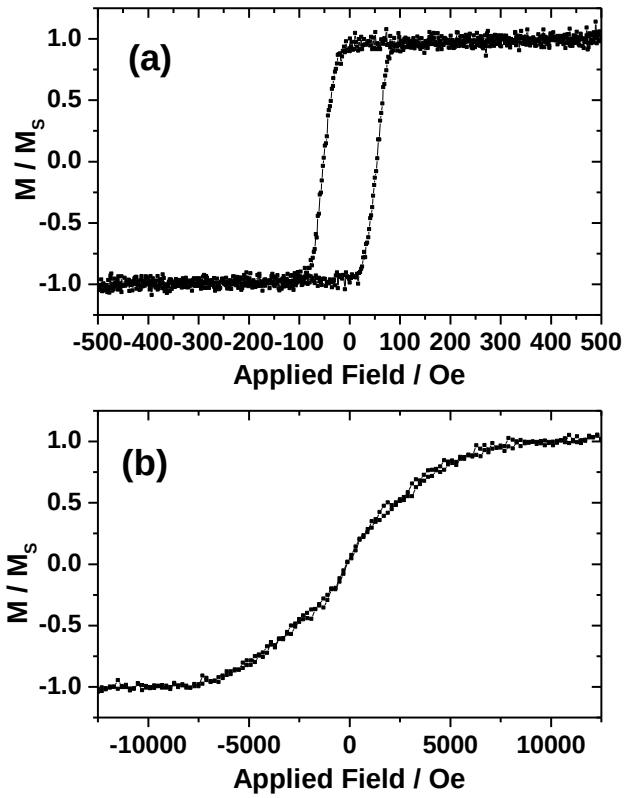

Figure 4.